Chem Rev Lett 8 (2025) 813-828

Research Article

Chemical Review and Letters
journal homepage: www.chemrevlett.com
ISSN (online): 2645-4947 (print) 2676-7279

NiCrAlY coatings on Inconel718LC super alloy via electrodeposition followed by post deposition annealing

Vahid Razmgir[1,] *

[1]*Department of Materials Engineering, Faculty of Mechanical Engineering, University of Tabriz, Tabriz, Iran.*

ARTICLE INFO

Article history:
Received 9 April 2025
Received in revised form 1 July 2025
Accepted 11 July 2025
Available online 30 July 2025

Keywords:
NiCrAlY metal interface coating, Nickel based superalloy (Inconel718LC), Electrochemical Deposition

ABSTRACT

The study investigated the fabrication of NiCoCrAlY intermediate coatings on Inconel 718LC nickel-based superalloy substrates using electrochemical deposition from a Watts bath containing NiCrAlY particles, followed by homogenization treatment. To achieve an optimal particle size, the initial NiCrAlY powder was mechanically milled under an argon atmosphere for 30 hours. The effects of NiCrAlY powder concentration in the electrodeposition bath and current density on the incorporation of co-deposited NiCrAlY particles and coating microstructure were examined. After deposition, the coatings were homogenized at 1100°C for 2 hours in an argon environment to ensure chemical uniformity. The chemical composition, phase structure, morphology, and hardness of the coatings were characterized using scanning electron microscopy (SEM), energy-dispersive X-ray spectroscopy (EDS), X-ray diffraction (XRD), and Microhardness testing. Results revealed that low powder concentrations and current densities resulted in limited incorporation of NiCrAlY particles, while increasing these parameters initially enhanced particle incorporation before eventual decline. Homogenization promoted the formation of γ'(Al_3Ni) intermetallic phases within the γ (Ni, Co) matrix. The increased incorporation of co-deposited particles improved hardness through solid solution strengthening, γ'(Al_3Ni) intermetallic phase formation, and microstructural refinement. The coating deposited at an optimal current density of 20 mA/cm^2 and NiCrAlY powder concentration of 20 g/l exhibited the highest hardness.

1. Introduction

MCrAlY (M = Ni, Co) interface coatings are widely employed as intermediate layers between superalloy substrates and ceramic thermal barrier coatings (TBCs) in gas turbines and aircraft engine components [1, 2]. Compared to other diffusion coatings, MCrAlY coatings offer greater compositional flexibility, enabling optimized coating properties. Additionally, their lower ductile-to-brittle transition temperature (DBTT) enhances their resistance to thermal cycling-induced cracking [3]. These coatings primarily serve to mitigate thermal mismatch stresses between the ceramic topcoat and superalloy substrate while providing protection against hot corrosion [4, 5].

However, the protective capability of these metallic coatings is not intrinsic; rather, it depends on their ability to form stable oxide scales. When exposed to oxygen, the coatings react to form dense, well-adhered oxide layers (Al_2O_3, Cr_2O_3) on the substrate surface. These layers act as barriers, preventing the infiltration of harmful elements (e.g., oxygen, nitrogen, sulfur) into the substrate [6]. To ensure continuous oxide formation, the coating must contain sufficient chromium, aluminum, and silicon. Both the coating composition and application method must be carefully selected to avoid two critical issues: (1) the formation of undesirable intermetallic phases, and (2) rapid interdiffusion of coating elements into the substrate.

* Corresponding author; e-mail:
https://doi.org/10.22034/crl.2025.515781.1574

Such phenomena can lead to porosity and crack formation at the coating-substrate interface. Moreover, elemental interdiffusion may deplete the coating's protective elements, compromising its long-term effectiveness. Ultimately, the service life of metallic coatings is determined by the stability and self-healing capacity of the oxide layer [7, 8].

MCrAlY coatings are extensively employed as intermediate layers on superalloy substrates in jet engine turbine blades and gas turbines [9]. While these coatings can be applied through various methods such as thermal spraying or physical vapor deposition, they are relatively costly and often unsuitable for components with complex geometries [10]. In contrast, electrochemical deposition has emerged as a prevalent technique for producing wear- and corrosion-resistant coatings [11]. However, few studies have investigated the electrochemical deposition of high-temperature coatings such as MCrAlY. Electrodeposition is a technique that utilizes fine powder dispersions in electrolytic solutions to produce multiphase composite coatings on substrates [12]. Since this method enables deposition from aqueous solutions with relatively low concentrations, it facilitates the formation of finer particles on the substrate surface [13, 14]. In addition to precise control over coating thickness, homogeneity, and deposition rate, this approach offers the advantage of producing dense, high-quality coatings [15].

Keller et al. developed a NiCrAlY composite coating and homogenized it at 1100℃ for 1–5 hours in a vacuum furnace [16]. Peng et al. fabricated a NiCrAlY/AlNiY composite coating, which formed a graded structure with an aluminum-rich outer layer and a chromium-rich inner layer after 4 hours of homogenization at 900°C under vacuum [17]. Zhang et al. employed electrochemical deposition to synthesize the NiCrAlY coating and subsequently investigated the effects of temperature on its morphology and elemental diffusion following 2 hours of homogenization [18].

This study aims to optimize the coating parameters for depositing NiCoCrAlY metallic coatings on a nickel-based superalloy substrate (Inconel 718LC) using electrochemical deposition. Specifically, we investigate the effects of homogenization treatment, current density, and NiCrAlY powder concentration in the electrodeposition bath on the microstructure and hardness of the NiCoCrAlY coatings.

2. Experimental procedures

2.1. Preparation of Samples

Table 1 presents the chemical composition of the nickel-based superalloy (Inconel 718LC) substrate used in this study. The substrate samples were machined using a Swiss-made Robofil 200 Charmilles robotic system and cut into rectangular cuboids with dimensions of 15 mm (length) × 10 mm (width) × 3 mm (thickness).

The samples underwent sequential preparation steps: sanding, degreasing, rinsing, acid washing, and final rinsing. Sanding was performed using SiC abrasive paper of varying grit sizes until all surface oxides and irregularities were removed at 800°C. Following sanding, the samples were cleaned with distilled water and acetone to eliminate residual oxides. For degreasing, the samples were immersed in an alkaline solution (NaOH, 140 g/L) at 60–70°C for 10 minutes with constant agitation, followed by distilled water rinsing. Surface activation was then conducted in an ultrasonic bath containing a 30 vol% hydrochloric acid solution at room temperature for 5 minutes. Prior to coating, all samples were thoroughly rinsed with distilled water.

2.2. Preparation of the initial powder

The initial powder material, Amdry 962 (Ni-22Cr-10Al-Y) supplied by Sulzer Metco, was produced via gas atomization. Table 2 presents its chemical composition. Due to the powder's large average particle size (80 μm), mechanical milling was performed at 180 rpm for 40 hours under argon atmosphere, using a ball-to-powder mass ratio of 1:10 to achieve size reduction. The resulting particles were then used to deposit Ni-Co/NiCrAlY composite alloy coatings on the nickel-based superalloy substrate.

Table 1. Percentage of elements and chemical composition of nickel base superalloy

Ni	Cr	Fe	Nb	Mn	Mo	S	Si
Balance	18.9	17.79	4.35	0.0372	3.02	0.0011>	0.108
V	W	Ta	Mg	Zr	Sb	Zn	Sn
0.0525	0.0141	0.0386	0.0088	0.0097	0.0015>	0.0071	0.0005>
C	Co	Al	Ti	Cu	B	P	As
0.0253	0.0674	0.45	0.969	0.048	0.0051	0.0129	0.002

Table 2. The chemical composition of the primary powder

Ni	Cr	Al	O	Y	H	N	Total Others	Acid Insoluble	Se
Balance	21.65	10.88	0.03	0.82	0.002	0.017	0.1>	0.02	0.005>

2.3. Deposition conditions

The Ni-Co/NiCrAlY composite alloy coatings were electrodeposited in a Watts bath containing NiCrAlY particles at concentrations specified in Table 3. The study investigated two key variables: (1) NiCrAlY powder concentration (10, 20, and 30 g/l) and (2) current density (10, 20, and 30 mA/cm^2), as outlined in Table 4. The first letter (A, B, C) indicates the applied current density level in mA per square centimeter: A: Current density of 10 mA/cm^2**,** B: Current density of 20 mA/cm^2 and C: Current density of 30 mA/cm^2. The subsequent number (10, 20, 30) represents the concentration of NiCrAlY powder in the electrolyte solution in grams per liter. Other deposition parameters — including bath temperature (45°C), pH (3.5), agitation rate (160 rpm), and coating duration (2 h) — were maintained constant based on established literature.

Table 3. Watts bath composition for electrochemical deposition

amount	Manufacturer	Role	chemicals
212.1 g/l	Merck	Nickel ion supply source	Nickel (II) sulfate
45.5 g/l	Merck	To increase the conductivity of the solution due to the presence of chlorine	Nickel (II) chloride
12.3 g/l	Merck	Cobalt ion supply source	Cobalt (II) sulfate
32.2 g/l	Sigma	As a buffer to keep the pH constant	Boric acid
0.2 g/l	Merck	Improving the quality of surface properties and reducing residual stress	SDS
10,20,30 g/l	Sulzer Metco	As composite particles	NiCrAlY

Table 4. Electrochemical deposition conditions

C (30 mA/cm^2)			B (20 mA/cm^2)			A (10 mA/cm^2)			current density
30	20	10	30	20	10	30	20	10	Concentration of NiCrAlY powder in the bath (g/l)
C_{30}	C_{20}	C_{10}	B_{30}	B_{20}	B_{10}	A_{30}	A_{20}	A_{10}	symbol

Homogenization was performed at 1100°C for 2 and 4 hours in a tube furnace (Model TF5/40–1250) under an argon atmosphere to dissolve NiCrAlY particles within the coating and achieve chemical homogeneity. Prior to furnace loading, samples were cleaned with alcohol to eliminate surface contaminants, and the furnace pressure was maintained at 2.5 bar at both ends.

To ensure the absence of oxygen and moisture in the process atmosphere, high-purity argon (≥ 99.999%) is used. Pure gases typically contain less than 1 ppm of oxygen and moisture. Additionally, purification systems such as oxygen traps and dryers are employed to remove impurities. Before entering the furnace, the gas passes through storage tanks for further purification. The oxygen level is continuously monitored in real time using precise sensors, and if it exceeds the allowable limit (usually < 10 ppm), an alarm system is activated.

To maintain an oxygen-free atmosphere in the furnace and prevent turbulent flows, the argon flow rate is precisely controlled. In small furnaces, the flow is typically set between 10 and 50 milliliters per minute. Accurate instruments such as mass flow controllers and vacuum-purge systems are used to minimize residual oxygen. The gas delivery system must be airtight, with devices like bubble counters at the outlet to ensure continuous flow. Additionally, samples may be covered with oxidation-resistant foils and placed in non-oxidizing ceramic crucibles to prevent oxidation. Finally, the absence of oxidation is verified using methods such as XRD, SEM/EDS, and TGA.

The selection of 1100°C for NiCrAlY homogenization is based on three key considerations: (a) Optimal formation of protective phases like β-NiAl, essential for developing stable Al_2O_3 oxide layers in thermal barrier coatings

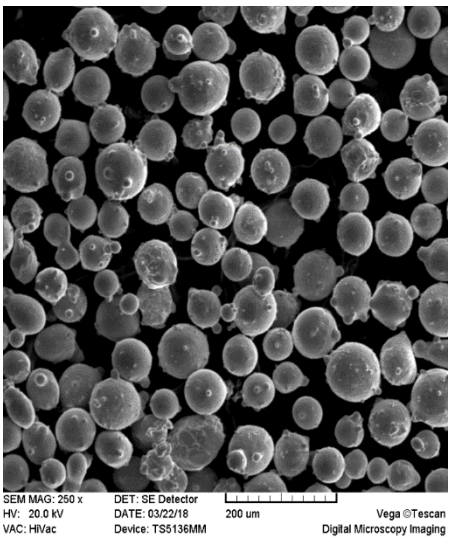

Fig .1. SEM image of NiCrAlY primary powder

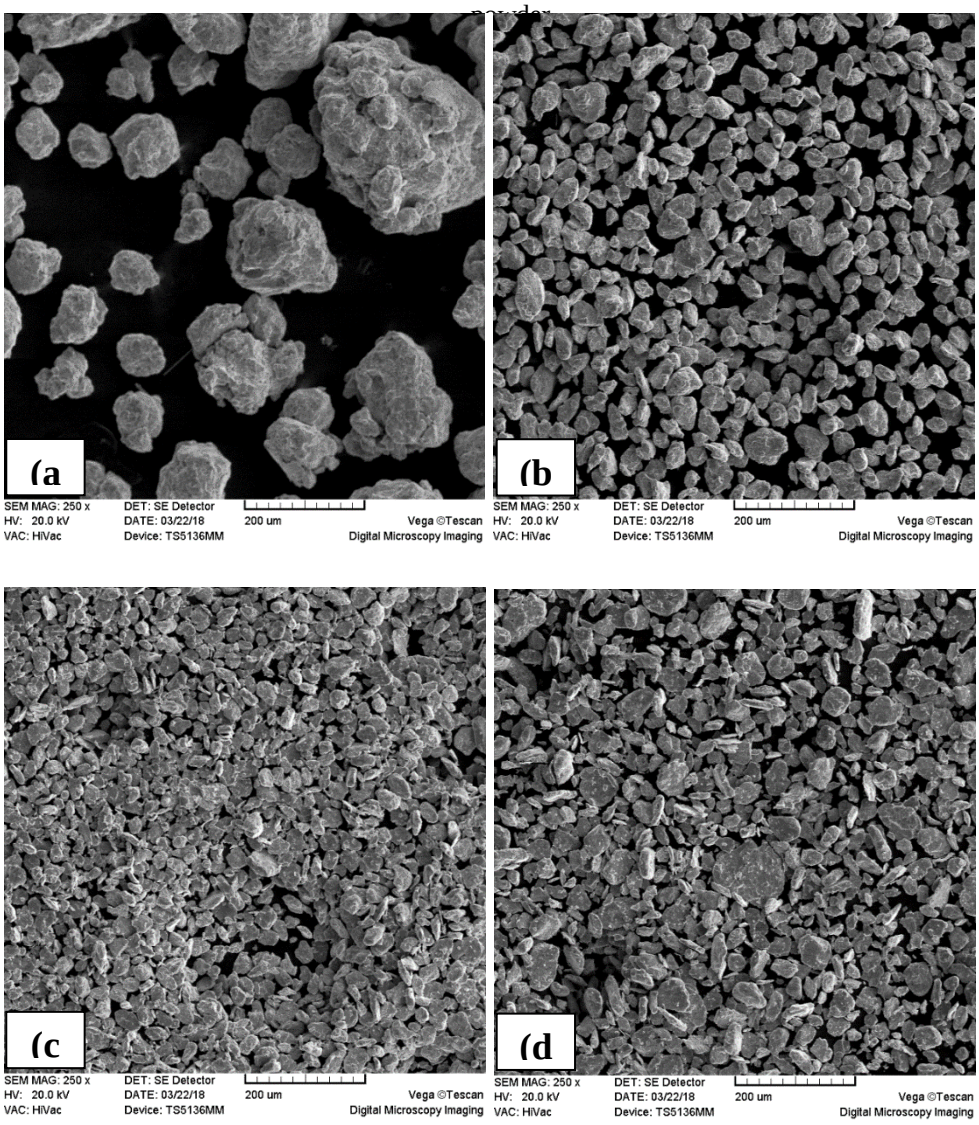

Fig. 2. SEM images of the mechanical milling process a) after 10 h, b) after 20 h, c) after 30 h, d) after 40 h

(TBCs) and oxidation-resistant coatings, while avoiding less protective phases (γ'-Ni_3Al or Cr-rich precipitates) that dominate at lower temperatures; (b) Enhanced atomic diffusion kinetics at 1100°C that ensure rapid homogenization of Al and Cr elements, whereas lower temperatures (<1100.°C) require impractically long processing times and risk chemical inhomogeneity; (c) Prevention of microstructural degradation, as higher temperatures (>1150°C) promote internal oxidation, porosity formation, and potential local melting of impurities, making 1100°C the optimal compromise between homogenization efficiency and microstructural stability.

2.4. Characterization

The coating microstructure was characterized using a CAMSCAN MV2300 scanning electron microscope (SEM; Czech Republic) to examine the morphology and structural features. Elemental distribution across the coating surface was analyzed through mapping, while linear and point analysis methods were employed to assess elemental distribution in cross-sections. Phase composition of the homogenized coatings was investigated using a Bruker D8 X-ray diffraction (XRD). Microhardness measurements were performed using an MDPEL-M400GL hardness tester. Due to surface roughness, measurements were conducted on sample cross-sections. Prior to testing, samples were mounted and polished to 2000-grit finish. The hardness testing protocol involved three measurements per cross-section at 3mm intervals under a 50 g load, with the average value reported as the sample hardness index.

3. Results and discussion

Figure 1 presents a scanning electron microscopy (SEM) image of the as-received powder, demonstrating its spherical particle morphology. The particle size distribution was analyzed using ImageJ software, revealing an average diameter of 80 μm with a range of 53-106 μm.

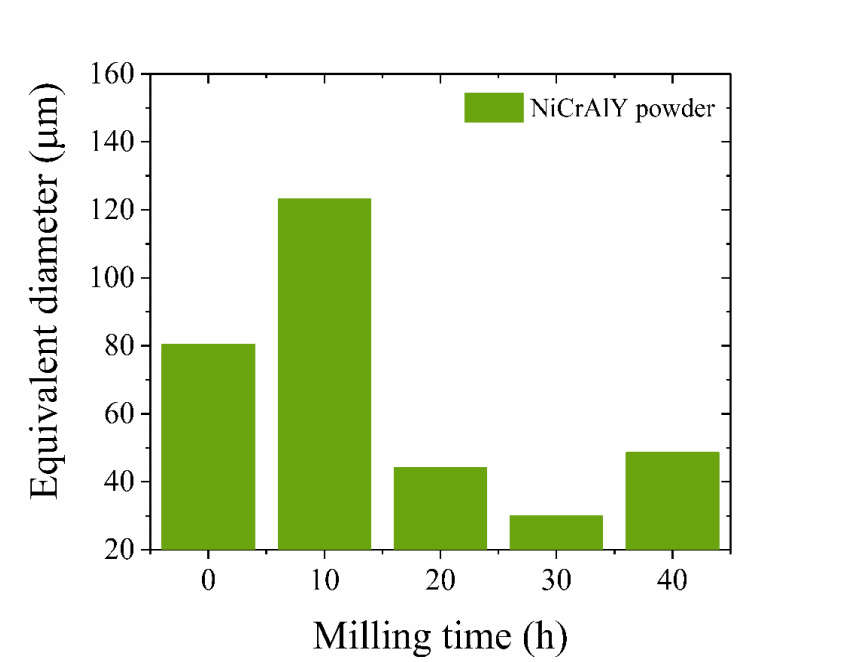

Figure 3. Changes in NiCrAlY particle size as a function of mechanical milling time.

Since smaller NiCrAlY powder was unavailable, the as-received powder was mechanically milled for varying durations to reduce particle size. Figure 2 presents SEM micrographs of the NiCrAlY powders after different milling periods.

Figure 3 displays the corresponding mean particle size evolution with milling time, as measured by ImageJ software. The SEM analysis reveals that particle agglomeration occurs during initial milling stages, leading to increased apparent particle size. However, extending the milling duration to 30 hours effectively reduces particle size. Further milling up to 40 hours results in a slight size increase due to particle cold welding. Consequently, 30 hours was identified as the optimal milling duration. All powders used for co-deposition were therefore milled for 30 hours.

Figure 4 presents the chemical composition analysis results for both the as-received powder and the mechanically milled powder after 30 hours. The NiCrAlY powder absorbed only 1 wt% oxygen during the 30-hour milling

process. Figure 5 displays the X-ray diffraction (XRD) patterns of the initial powder compared with the 30-hour milled powder. Three distinct phases were identified in the initial powder: γ (Ni, Cr-rich) phase, γ' (Ni_3Al) phase, and β (NiAl) phase, consistent with previous reports on NiCrAlY powders [19-26]. Following mechanical milling, only these primary phase peaks remain visible, with no detectable oxide-phase peaks. Combined with EDS analysis, these results demonstrate that NiCrAlY particles undergo minimal oxidation during mechanical milling.

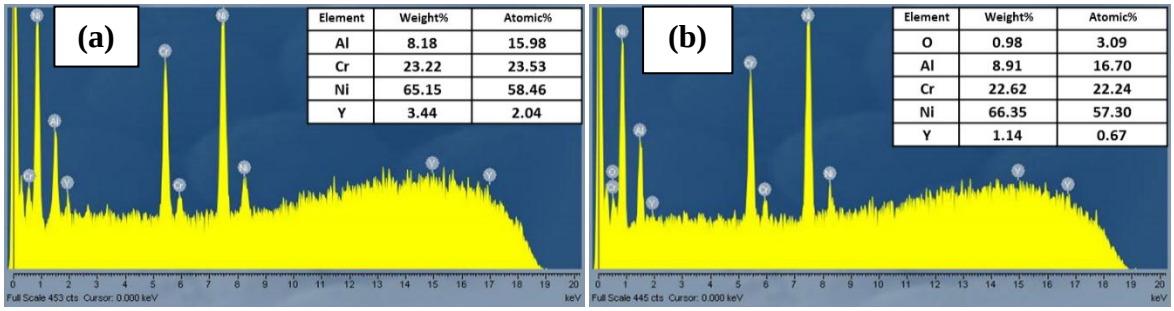

Fig. 4. EDS test results a) Primary powder b) Powder after 30 h ball milling.

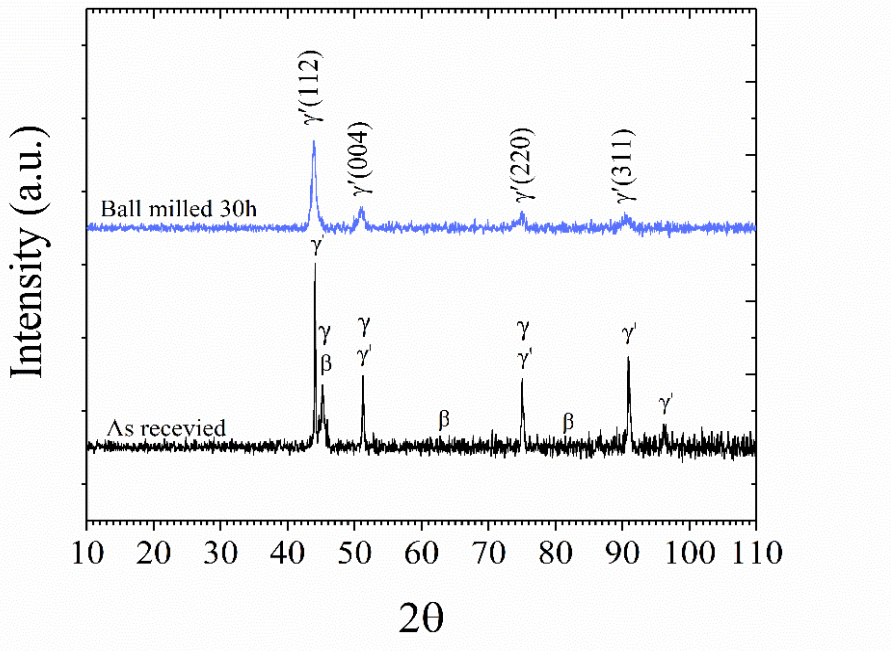

Fig. 5. XRD dispersion patterns of primary powder and ball milled powder for 30 h.

The three X-ray scattering patterns of the primary powder and the powder ball-milled for 30 hours reveal that after mechanical processing, the intensity of the scattering peaks decreased while their width increased. The increase in peak width indicates a reduction in the crystal size within each powder particle. The overlapping and broadening of the scattering peaks result from the simultaneous increase in peak width and decrease in peak intensity.

To produce NiCoCrAlY coatings from the deposited composite coatings, a homogenization treatment is necessary. According to previous studies, the coated samples were homogenized in argon gas at 1100°C for 2 or 4 hours [16, 20]. Figure 6 presents the changes in the chemical composition of the coating after homogenization, as determined by EDS line scan analysis at a current density of 20 mA/cm^2 and a NiCrAlY powder concentration of 20 g/l. It can be observed that the chromium content decreases significantly from the coating's interior toward the surface.

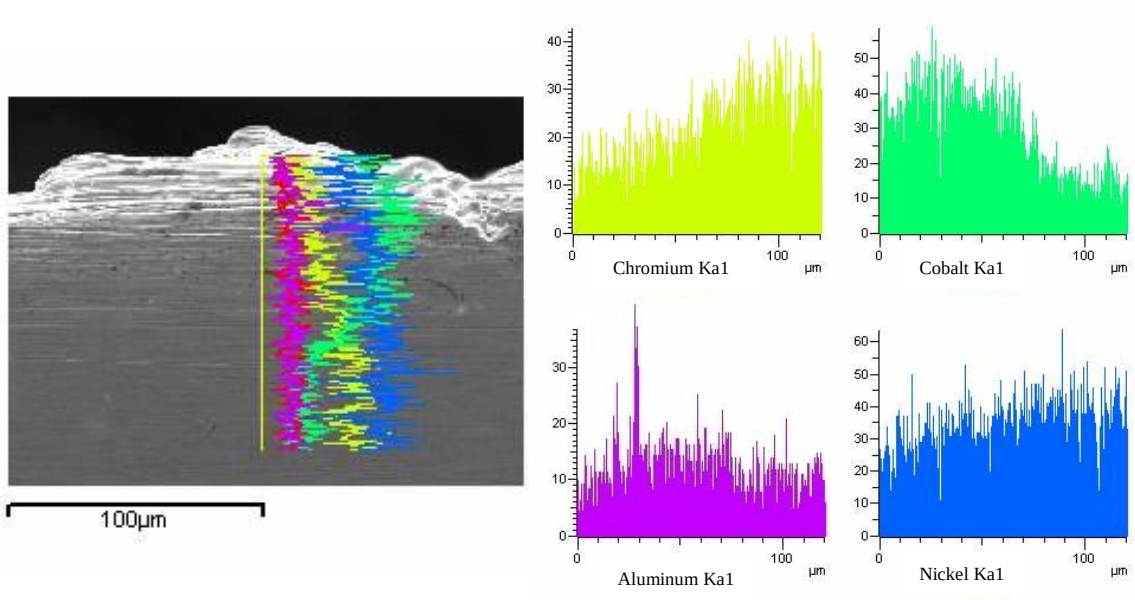

Fig. 6. Results of linear analysis of the cross section of NiCoCrAlY coating at a current density of 20 mA/cm^2 and at a powder concentration of 20 g/l after 4 h of the homogenization operation.

Figure 7 presents the numerical results of point EDS analysis for coatings deposited at different NiCrAlY particle concentrations, along with the density of various sedimentation streams after 4 hours of homogenization. These analyses were conducted to determine the precise chemical composition of the coatings. Following 4 hours of homogenization, minor variations in the chromium and aluminum content of the coatings were observed, depending on both the current density and the NiCrAlY powder concentration in the electrodeposition bath. The chromium and aluminum content initially increases and then decreases with rising current density for powder concentrations of 10 g/l, 20 g/l, and 30 g/l. The maximum concentration was achieved at a current density of 20 mA/cm^2 and a powder concentration of 20 g/l.

At low current densities (e.g., 10 mA/cm^2), the hydrodynamic force is sufficient for effective deposition and adsorption of NiCrAlY particles onto the cathode surface, but the resulting chromium and aluminum content in the coating remains lower than that obtained at 20 and 30 mA/cm^2. Consequently, when the aluminum content in the coating falls below 6 wt%, the coating cannot form a homogeneous protective oxide layer at the interface. This leads to rapid coating degradation under high-temperature oxidizing conditions [21]. Thus, a current density of 10 mA/cm^2 is unsuitable for producing a functionally adequate coating. Although an increase in chromium and aluminum content was expected at higher current densities due to changes in suspension stability and particle agglomeration, the observed values instead decreased compared to those obtained at 20 mA/cm^2 [22-26].

Due to the significant reduction in chromium and aluminum concentrations during the 4-hour homogenization process, coatings produced at current densities of 20 and 30 mA/cm^2 with NiCrAlY powder concentrations of 10, 20, and 30 g/l underwent a shorter 2-hour homogenization treatment in an argon atmosphere at 1100°C. These findings are supported by quantitative EDS point analysis of the cross-sectional elemental composition of the NiCoCrAlY coatings after the 2-hour homogenization. Figure 8 illustrates the percentage changes in chromium and aluminum content within the coatings after 2 hours of homogenization as a function of both current density and powder concentration in the electrodeposition bath. The data reveal that chromium and aluminum levels increase following the shorter homogenization period compared to the 4-hour treatment. The analysis demonstrates that as current density increases across all powder concentrations (10, 20, and 30 g/l), the chromium and aluminum content decreases. This occurs because higher current densities enhance powder incorporation into the coating, thereby increasing the weight percentage of chromium and aluminum - key elements that improve oxidation resistance and hot corrosion performance. However, excessively high current densities compromise suspension stability and promote particle agglomeration, ultimately reducing the beneficial element content.

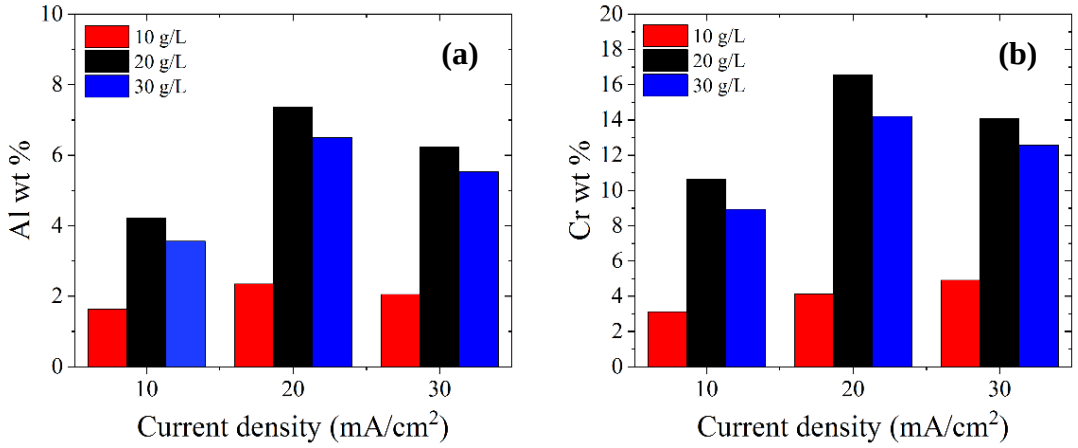

Fig. 7. Percentage changes a) aluminum b) chromium in NiCoCrAlY coating after 4 h homogenization operation at three current densities of 10, 20, 30 mA/cm2 and at three concentrations of NiCrAlY powder, 10, 20, 30 g/l at 1100°C.

Furthermore, the concentration of NiCrAlY particles in the electrodeposition bath significantly affects the powder content in the coating. At low concentrations, the interparticle distance is large, resulting in fewer collisions despite bath agitation. As the particle concentration increases, both the collision probability and the likelihood of particle coalescence rise correspondingly. Additionally, higher particle concentrations enhance the probability of particles impacting either the cathode surface or the growing coating, thereby increasing their incorporation into the coating structure. However, excessive particle concentration promotes the formation of coarse agglomerates more than it facilitates particle attachment to the cathode surface, ultimately reducing the effective powder deposition rate. The optimal balance is achieved at a current density of 20 mA/cm^2 with a powder concentration of 20 g/l, which yields the highest chromium and aluminum content in the coating.

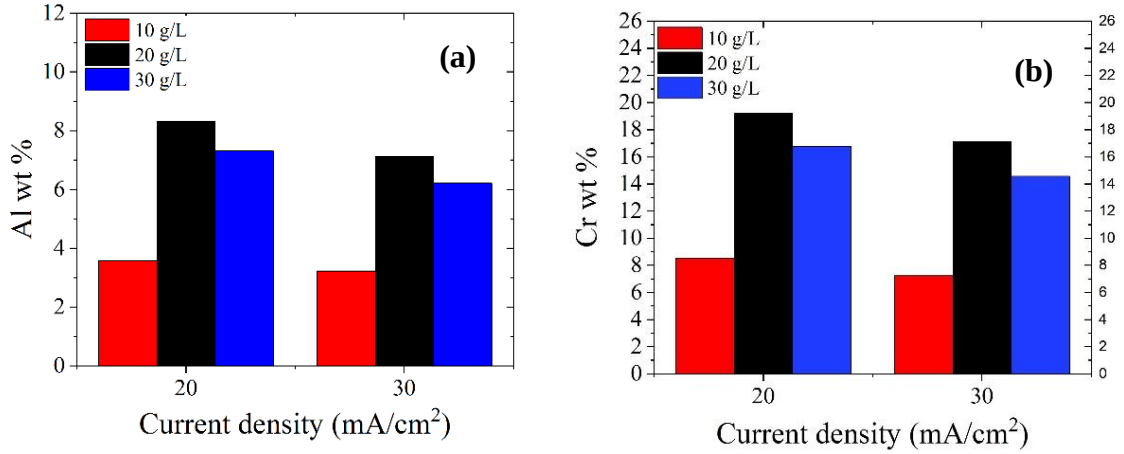

Figure 8. Percentage changes a) aluminum b) chromium in NiCoCrAlY coating after 2 h homogenization operation at two current densities of 20, 30 mA/cm^2 and in three concentrations of NiCrAlY powder, 10, 20, 30 g/l at 1100°C.

Figure 9 presents the surface morphology of the coated superalloy following 2 hours of homogenization at 20 mA/cm^2 with a powder concentration of 20 g/l. The coating maintains most of its original roughness and silver coloration after argon atmosphere homogenization, indicating no significant surface oxidation occurred during the process. Figure 10 displays a SEM micrograph of the NiCoCrAlY coating surface in its as-deposited state (prior to homogenization) at the same current density (20 mA/cm^2) and powder concentration (20 g/l). The surface exhibits a characteristic cauliflower-like morphology with noticeable roughness.

magnification images of coatings processed under different conditions reveal the formation of cavities and pores during

Fi. 9. Macroscopic image of NiCoCrAlY metal interface coating surface after 2 h homogenization operation at a current density of 20 mA/cm^2 and a concentration of NiCrAlY powder of 20 g/l at 1100°C.

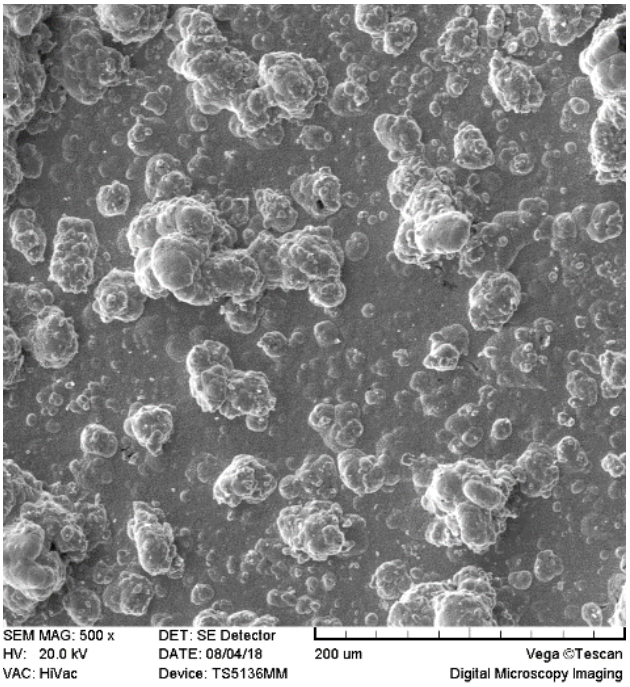

Figure 10. Scanning electron microscope image of NiCoCrAlY metal interface coating surface before 2 h homogenization operation at current density of 20 mA/cm^2 and concentration of NiCrAlY powder, 20 g/l at 1100°C.

Figure 11 presents scanning electron microscopy (SEM) images of NiCoCrAlY coating surfaces after 2-hour homogenization at 1100°C, shown at two different magnifications. Following homogenization, the surface morphology exhibits significant changes, with previously distinct edges and corners becoming smoothed. High-homogenization. These features can be attributed to: Density variations among elements in NiCrAlY particles (consistent with the Kirkendall effect), and other contributing factors. Table 5 [18] provides quantitative data on the density differences between various phases formed by NiCrAlY particles and the (Ni, Co) matrix.

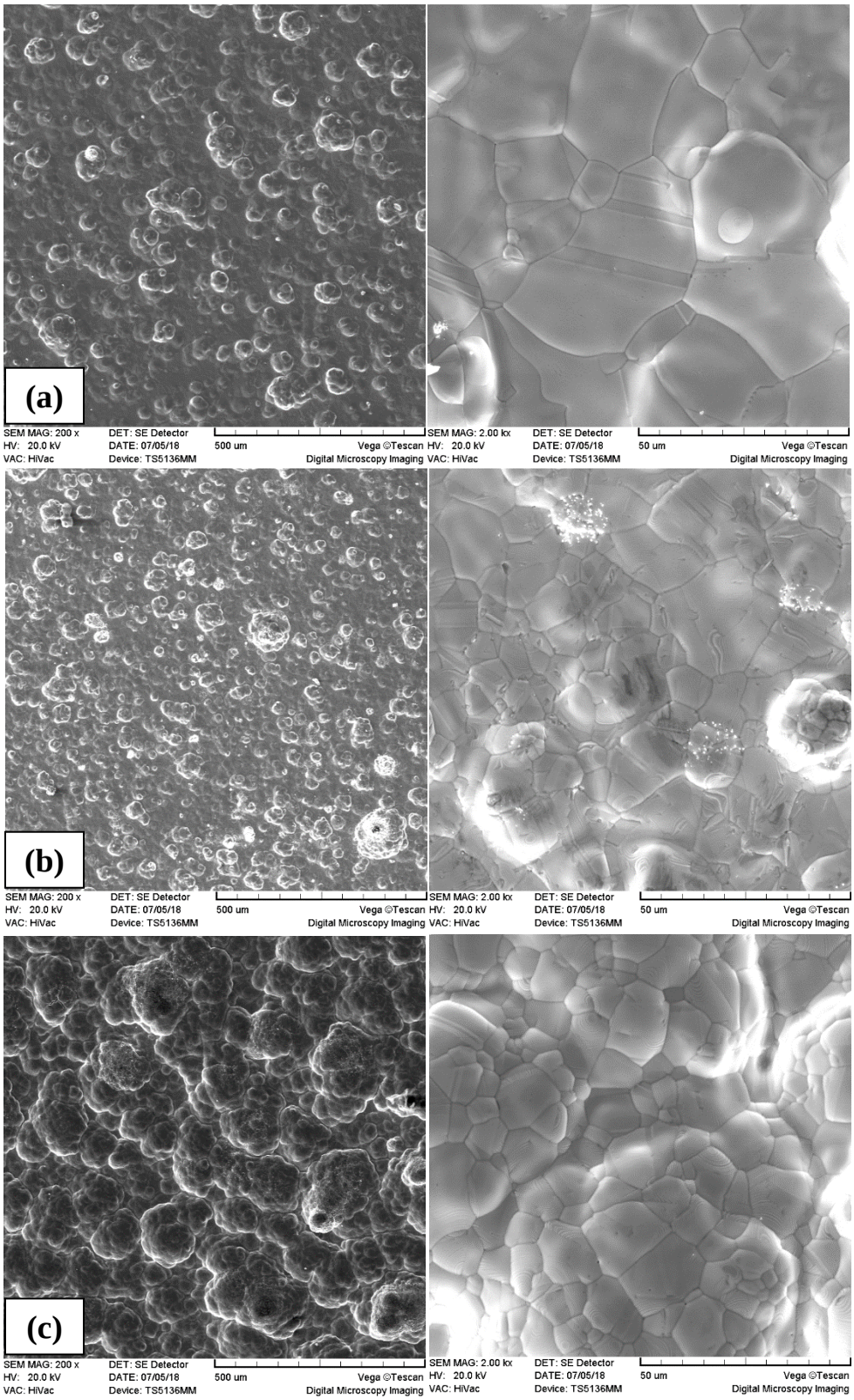

Figure 11. Surface morphology of NiCoCrAlY coatings after 2 h homogenization operation at 1100°C in a) B_{10}, b) C_{10}, c) B_{20}, d) C_{20}, e) B_{30}, and) C_{30}.

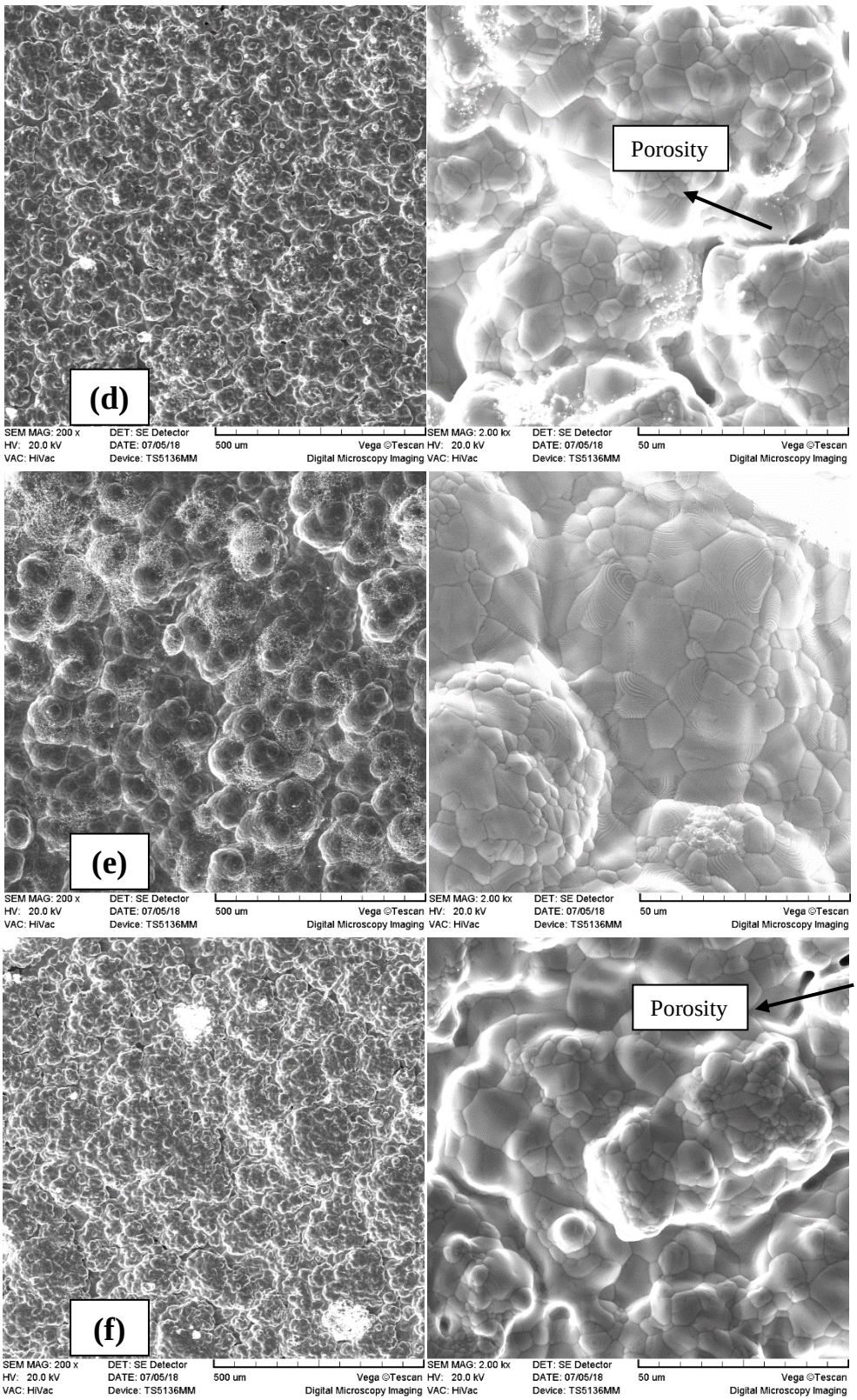

Continuation of Fig. 11

Table 5. Density of NiCoCrAlY coating phases

	Ni-Co field coating	NiCrAlY particles	NiAl	Ni_3Al
Density (g/cm^3)	8.9	4.5	5.9	7.5

The coating morphology improves with increasing current density, likely due to enhanced powder incorporation into the coating. Scanning electron microscopy (SEM) analysis confirms that higher current densities yield a more refined coating morphology. These observations can be explained by the increased presence of NiCrAlY particles, which serve as: Nucleation sites, and Growth barriers, resulting in a more granular coating structure.

Figure 12 presents a cross-sectional scanning electron microscopy (SEM) image of the coated sample following 2-hour homogenization. Energy-dispersive X-ray spectroscopy (EDS) analysis (Scheme 13) reveals that the NiCoCrAlY coating microstructure contains dark regions corresponding to aluminum oxide inclusions. Under these processing conditions, the average coating thickness measures approximately 80 μm.

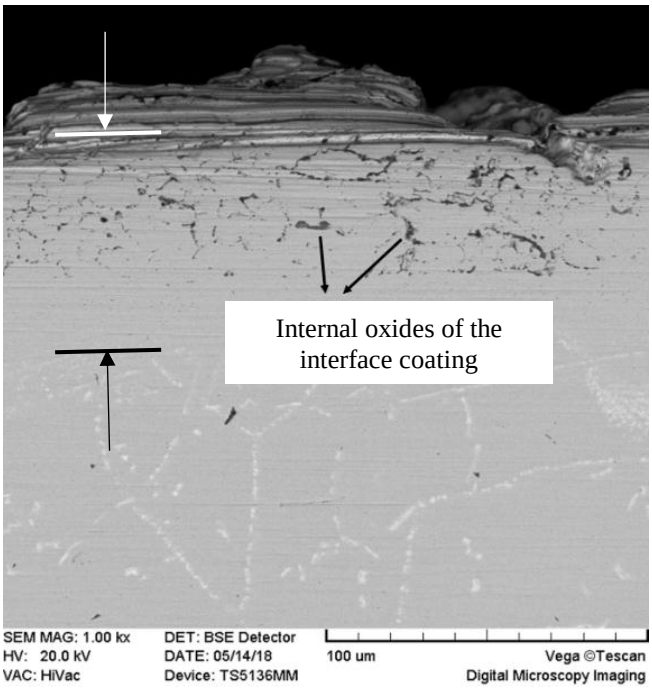

Fig. 12. SEM cross-sectional image of the sample including substrate and interface coating. NiCoCrAlY

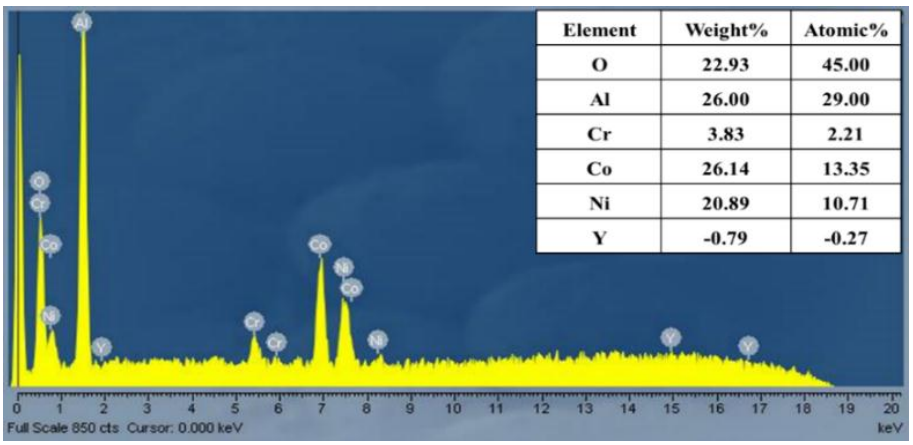

Fig. 13. EDS test results from black lines and surrounding areas.

Figure 14 presents a scanning electron microscopy (SEM) image of the coated sample surface after 2 hours of homogenization. The image reveals that the NiCoCrAlY coating interface exhibits a characteristic beach-like microstructure, the term 'beach-like microstructure' has likely been adopted due to self-organization mechanisms similar to cellular structures, including cooperation between adjacent regions to minimize surface energy. In cellular structures, boundaries form based on differences in growth direction or chemical composition, and if growth occurs in a branching manner, it may partially resemble dendritic structures. However, the 'beach-like' designation primarily refers to the continuous, wavy pattern rather than dendritic tree-like branching. This morphology probably results from non-uniform phase distribution or localized variations in oxidation and evaporation during thermal processing, leading to the formation of alternating light and dark regions (in SEM images) - similar to wave patterns on beach sands. Thus, these terminologies are justified based on their morphological characteristics and formative processes.

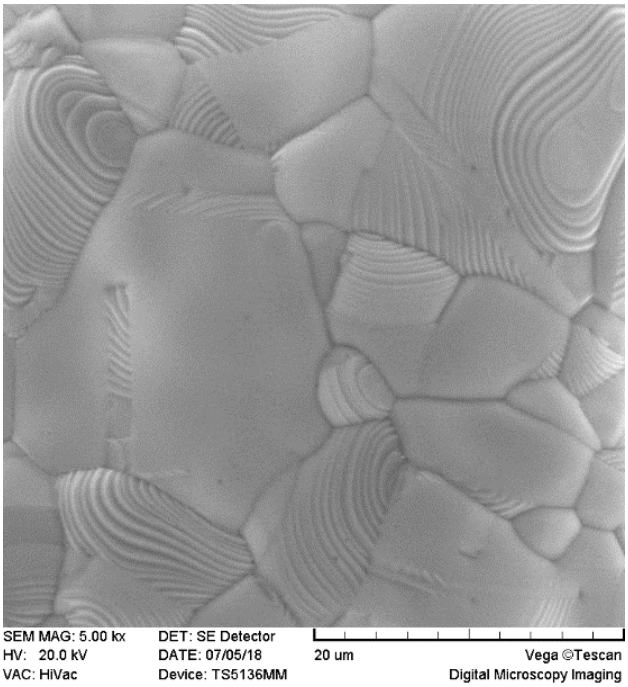

Fig. 14. Surface morphology of NiCoCrAlY coatings after 2 h homogenization operation at 1100°C in high magnification.

Figure 15 presents the X-ray diffraction (XRD) pattern of NiCoCrAlY coatings after 2-hour homogenization at 1100°C. A comparison of diffraction patterns between coatings produced from initial powder and 30-hour milled powder reveals the formation of both β and γ phases in the coating structure. Notably, the γ' phase diffraction peaks show increased intensity relative to those observed in the milled powder.

Previous studies [18] indicate that during homogenization, NiCrAlY particles completely dissolve into the nickel-cobalt matrix. This process, accompanied by interdiffusion, leads to the formation of γ'-Ni_3Al, β-NiAl, and γ-Ni (Cr-rich) phases. However, following homogenization, the β and γ peaks do not appear in the XRD pattern because the β phase is an intermetallic compound with an ordered structure. During homogenization, aluminum (Al) becomes uniformly distributed throughout the matrix, disrupting the ordered NiAl structure. Consequently, β crystals are no longer sufficiently large or ordered to produce distinct X-ray diffraction peaks. Furthermore, the γ phase is essentially an FCC solid solution of Ni and Co. After homogenization, Ni and Co atoms become uniformly distributed within the lattice, resulting in no detectable differences in XRD diffraction patterns.

Post-homogenization, the γ' phase emerges as the dominant peak in XRD patterns due to its higher stability and more distinct crystallization. This phenomenon is particularly evident at the optimal powder concentration (20 g/l), where the intensity of γ' and β peaks reaches its maximum. The reduced chromium content (resulting from evaporation) and aluminum diffusion into the substrate may also contribute to the diminished presence of other phases.

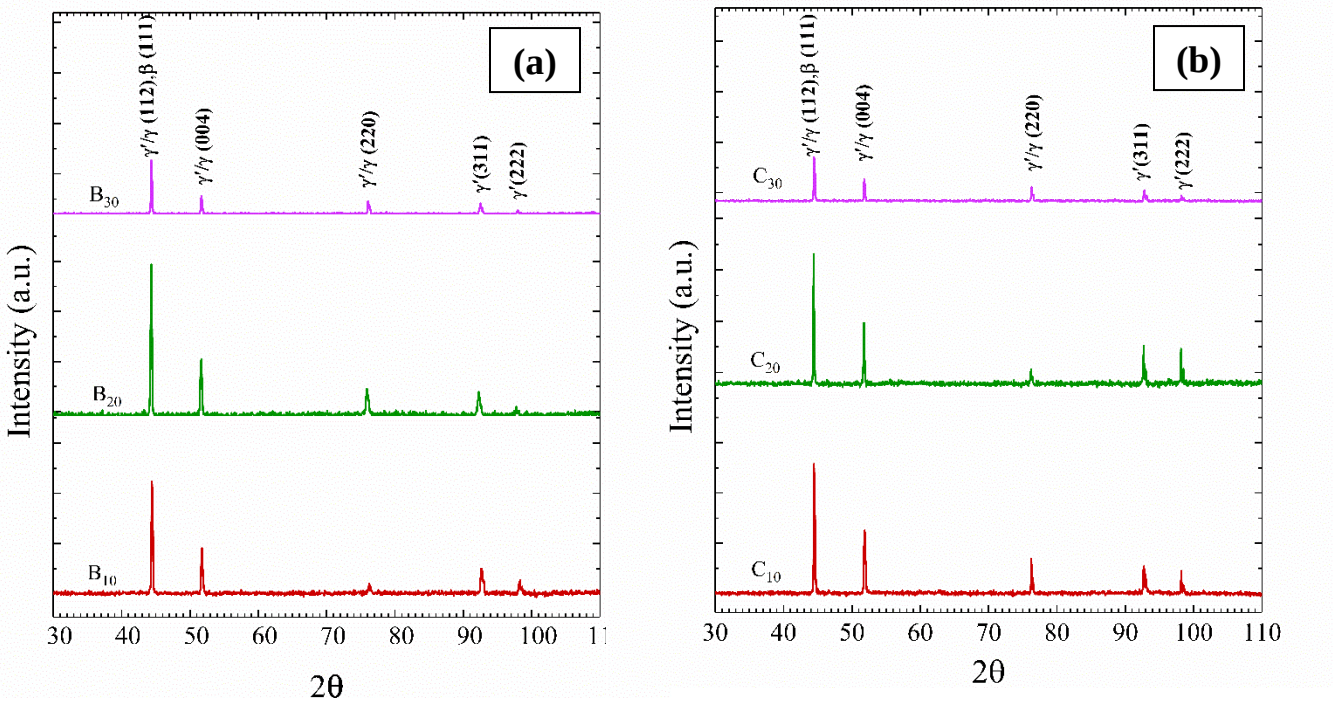

Fig. 15. XRD test results of NiCoCrAlY coatings a) current density of 20 mA/cm^2 in three concentrations of powder 10-30-20 g/l b) current density of 30 mA/cm^2 in three concentrations of powder 30-30-20 g/l.

Figure 16 presents the cross-sectional hardness profile of NiCoCrAlY coatings following 2-hour homogenization at 1100°C. The results demonstrate that increasing the powder concentration in the electrodeposition bath enhances sample hardening. This strengthening effect arises from: The formation of γ'-Ni_3Al phase following homogenization at 1100°C plays a key role in enhancing the coating's hardness and strength. This intermetallic phase, with its ordered structure and strong bonds, acts as an effective reinforcement in the (γ-Ni, Cr) matrix. XRD results demonstrate that under optimal conditions (20 mA/cm^2 current density and 20 g/l powder concentration), the intensity of γ' phase peaks reaches its maximum, indicating enhanced formation of this hard phase. Furthermore, the high coherence between the γ' phase and matrix, along with the formation of reinforcing nanoparticles, contributes to a significant increase in hardness.

Table 6 shows the grain size measurements obtained using the Debye-Scherrer method. According to the Hall-Petch relationship, under optimal conditions (20 g/l and 20 mA/cm^2), reduced grain size leads to increased hardness. However, increasing powder concentration beyond 30 g/l results in particle agglomeration and porosity formation, which reduces hardness. Additionally, other mechanisms such as solid solution strengthening (due to dissolution of NiCrAlY particles in the nickel-cobalt matrix) and the Kirkendall effect (caused by phase density differences and resulting internal stresses) also significantly affect the coating's mechanical properties.

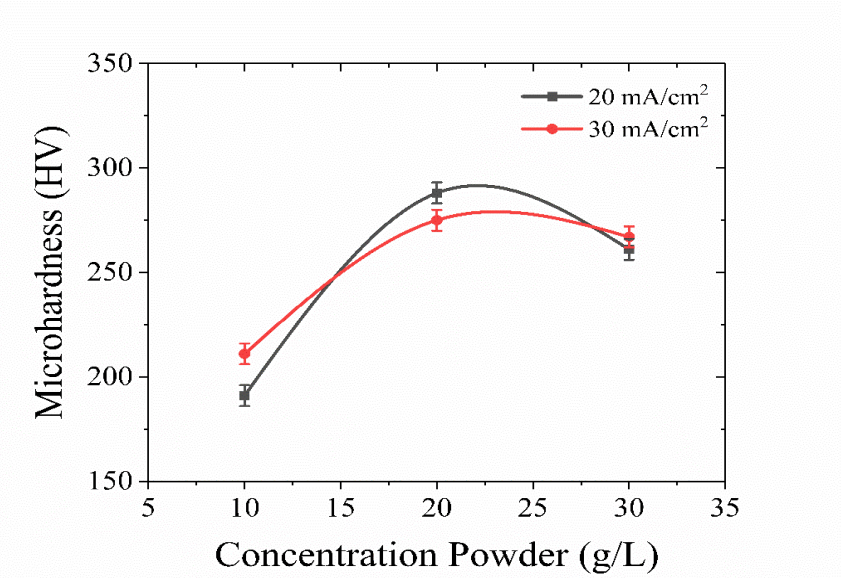

Fig. 16. Micro hardness diagram of NiCoCrAlY coating.

Table 6. Grain size values calculated by Debay Scherer method for NiCoCrAlY coatings

Sample	Grain size (Å)	Sample	Grain size (Å)
B_{10}	651.91	C_{10}	768.59
B_{20}	461.92	C_{20}	695.41
B_{30}	623.19	C_{30}	712.73

4. Conclusions

Ni-Co/NiCrAlY composite alloy coatings containing 35-40 vol% NiCrAlY particles were fabricated on Inconel 718LC nickel-based superalloy via electrochemical deposition. Post-deposition heat treatment under argon atmosphere significantly influenced the microstructure and chemical composition of the resulting NiCoCrAlY coatings. The heat-treated coatings exhibited an average composition of Ni-(14-18)Co-(14-18)Cr-(6-8)Al (wt%). These findings suggest that heat treatment temperatures should remain below 1100°C to: Minimize chromium evaporation and Prevent diffusion of detrimental elements from the substrate to the coating surface. Electrodeposition analysis revealed that: Low current densities yield limited NiCrAlY particle incorporation, increased current density enhances powder deposition but causes coating irregularity and higher powder concentrations promote particle collisions in the bath, hindering effective co-deposition. The optimal processing parameters were determined to be 20 mA/cm^2 current density with 20 g/l NiCrAlY powder concentration. This condition maximizes coating hardness through: Solid solution strengthening, Formation of γ' (Al_3Ni) intermetallic precipitates within the γ (Ni, Co) matrix and Microstructural refinement. The peak hardness was achieved at these optimal parameters, demonstrating the importance of balanced processing conditions.

5. References

[1] A. Gil, V. Shemet, R. Vassen, M. Subanovic, J. Toscano, D. Naumenko, L. Singheiser, W.J. Quadakkers, Effect of surface condition on the oxidation behaviour of MCrAlY coatings. Surface and Coatings Technology, 201. 7 (2006), 3824-3828. doi:10.1016/j.surfcoat.2006.07.252.

[2] J. Wang, H., Ji, M. Chen, Z. Bao, S. Zhu, F. Wang, High temperature oxidation and interdiffusion behavior of recoated NiCoCrAlY coating on a nickel-based superalloy. Corrosion Science, 175 (2020), 108894. https://www.sciencedirect.com/science/article/pii/S0010938X20307563.

[3] D. Texier, D. Monceau, Z. Hervier, E. Andrieu, Effect of interdiffusion on mechanical and thermal expansion properties at high temperature of a MCrAlY coated Ni-based superalloy. Surface and Coatings Technology, 307 (2016), 81-90. http://dx.doi.org/10.1016/j.surfcoat.2016.08.059.

[4] Y.F. Yang, P. Ren, Z.B. Bao, S.L. Zhu, F.H. Wang, W. Lia, Effect of Pt-rich position on the hot corrosion behavior of NiCoCrAlY coating for a single-crystal superalloy. Surface and Coatings Technology, 395 (2020), 125938. https://www.sciencedirect.com/science/article/pii/S0257897220306071.

[5] Q.M. Wang, Y.N. Wu, P.L. Ke, H.T. Cao, J. Gong, C. Sun, L.S. Wen, Hot corrosion behavior of AIP NiCoCrAlY (SiB) coatings on nickel base Superalloy. Surface & Coatings Technology, 186.3 (2004), 389-397.

https://www.sciencedirect.com/science/article/pii/S0257897204000167.

[6] P. Puetz, X. Huang, R.S. Lima, Q. Yang, L. Zhao, Characterization of transient oxide formation on CoNiCrAlY after heat treatment in vacuum and air. Surface & Coatings Technology, 205. 2 (2010), 647-657. https://www.sciencedirect.com/science/article/pii/S0257897210006018.

[7] M. Bahamirian, Sh. Khameneh ASL, An Investigation on effect of bond coat replacement on hot corrosion properties of thermal barrier coatings. Iranian Journal of Materials Science and Engineering, 10. 3(2013), 12-21.

[8] H.J. Zhang, Oxidation and hot corrosion of electrodeposited Ni–7Cr–4Al nanocomposite. Transactions of Nonferrous Metals Society of China, 25. 1 (2015), 191-198. https://www.sciencedirect.com/science/article/pii/S1003632615635956.

[9] Y. Chen, X. Zhao, M. Bai, L. Yang, C. Li, L. Wang, P. Xiao, A mechanistic understanding on rumpling of a NiCoCrAlY bond coat for thermal barrier coating applications. Acta Materialia, 128 (2017), 31-42. https://doi.org/10.1016/j.actamat.2017.02.003.

[10] R. Sobhanverdi, A. Akbari, Porosity and microstructural features of plasma sprayed Yttria stabilized Zirconia thermal barrier coatings. Ceramics International, 41 (2015), 14517-14528. https://www.sciencedirect.com/science/article/pii/S0272884215013929.

[11] H. Zhen, X. Peng, A new approach to manufacture oxidation-resistant NiCrAl overlay coatings by electrodeposition. Corrosion Science, 150 (2019), 121-126. https://www.sciencedirect.com/science/article/pii/S0010938X18316524.

[12] F.C. Walsh, C. Ponce de Leon, A review of the electrodeposition of metal matrix composite coatings by inclusion of particles in a metal layer: an established and diversifying technology, Trans. Inst. Met. Finish, 92. 2 (2014), 83-98. DOI 10.1179/0020296713Z.000000000161.

[13] B.L. Bates, L.Z. Zhang, Y. Zhang, Electrodeposition of Ni matrix composite coatings with embedded CrAlY particles, Surf. Eng. 31. 3 (2015), 202-208. https://doi.org/10.1179/1743294414Y.0000000376.

[14] B.L. Bates, J.C. Witman, Y. Zhang, Electrolytic codeposition of Ni-CrAlY composite coatings using different deposition configurations. Materials and Manufacturing Processes, 31. 9 (2016), 1232-1237. https://doi.org/10.1080/10426914.2015.1090596.

[15] J. Forster, B.P. Cameron, J.A. Carews, The production of multi-component alloy coatings by particle co-deposition, Trans. Inst. Met. Finish. 63. 1 (1985), 115-119. https://doi.org/10.1080/00202967.1985.11870719.

[16] I. Keller, D. Naumenko, W.J. Quadakkers, R. Vaßen, L. Singheiser, Influence of vacuum heat treatment parameters on the surface composition of MCrAlY coatings. Surface & Coatings Technology, 215 (2013), 24-29. http://dx.doi.org/10.1016/j.surfcoat.2012.09.066.

[17] X. Peng, S. Jiang, J. Gong, X. Sun, C. Sun, Preparation and Hot Corrosion Behavior of a NiCrAlY + AlNiY Composite Coating. Journal of Materials Science & Technology. 32. 6 (2016), 587-592. https://www.sciencedirect.com/science/article/pii/S1005030216300548.

[18] L.Z. Zhang, B.L. Bates, Y. Zhang, Effect of post-deposition heat treatment on electrodeposited NiCoCrAlY coatings. Materials Science and Engineering for Energy Systems, 11. 2 (2016), 136-141. https://doi.org/10.1080/02670844.2016.1198451.

[19] J.A. Picas, A. Forn, L. Ajdelsztajn, J. Schoenung, Nanocrystalline NiCrAlY powder synthesis by mechanical cryomilling. Powder Technology, 148. 1 (2004), 20-23. doi:10.1016/j.powtec.2004.09.015.

[20] T. J. Nijdam, L.P.H. Jeurgens, J. H. Chen, W.G. Sloof, On the Microstructure of the Initial Oxide Grown by Controlled Annealing and Oxidation on a NiCoCrAlY Bond Coating. Oxidation of Metals, 64 (2005), 355-377. https://doi.org/10.1007/s11085-005-8532-6.

[21] Q.M. Wang, Y.N. Wu, M.H. Guo, P.L. Ke, J. Gong, C. Sun, L.S. Wen, Ion-plated Al–O–N and Cr–O–N films on Ni-base superalloy as diffusion barriers. Surface & Coatings Technology, 197 (2005), 68-76. https://www.sciencedirect.com/science/article/pii/S0257897204009077.

[22] M.S. Mehr, A. Akbari,, E. Damerchi, Electrodeposited Ni-B/SiC micro- and nano-composite coatings: A comparative study. Journal of Alloys and Compounds, 782 (2019), 477-487. https://doi.org/10.1016/j.jallcom.2018.12.184.

[23] A. K. Nomozov, Kh. S. Beknazarov, N. B. Chorieva, Kh. Ch. Mirzakulov, K. S. Arifdjanova, A. S. Mukimov, A. A. Pardaev, N. D. Ashurova, Recent developments in polymer-based composite anticorrosion coatings: Materials, mechanisms and applications. International Journal of Corrosion and Scale Inhibition, 14 (2025) 1362–1390. doi:10.17675/2305-6894-2025-14-3-18.

[24] K. Nomozov, Kh. S. Beknazarov, Y. A. Geldiev, B.E. Babamurodov, N. Sh. Muzaffarova, S. G. Yuldashova. Synthesis of PFG brand corrosion inhibitor and its quantum chemical calculation results. Chemical problems 3 (2025) 297-309. https://doi.org/10.32737/2221-8688-2025-3-297-309.

[25] Z. K. Misirov, K. S. Beknazarov. Synthesis and application of corrosion inhibitor for hydrogen sulfide corrosion of steel. Indian Journal of Chemical Technology, 32 (2023) 101–109. https://doi.org/10.56042/ijct.v32i3.7278.

[26] A. Nomozov, Khs. Beknazarov, B. A. Normurodov, Z. Kh. Misirov, S. G. Yuldashova, G. J. Mukimova, D. A. Nabiev, Z. Jumaeva, Inhibition potential of Salsola oppositifolia extract as a green corrosion inhibitor of mild steel in an acidic solution. Int J Corros Scale Inhib. 14 (2025) 1103–1115. https://doi.org/10.17675/2305-6894-2025-14-3-5.